Materials Science and Engineering, A168 (1993) 55–59

The role of nitrogen in the intergranular glass phase of Si_3N_4 on high temperature applications and wear

R. F. Silva and A. P. Moreira
Departamento de Engenharia Cerâmica e do Vidro, Universidade de Aveiro, 3800 Aveiro (Portugal)

J. M. Gomes and A. S. Miranda
Departamento de Engenharia Mecânica, Universidade do Minho, 4800 Guimarães (Portugal)

J. M. Vieira
Departamento de Engenharia Cerâmica e do Vidro, Universidade de Aveiro, 3800 Aveiro (Portugal)

Abstract

The hot hardness of Si_3N_4 tool materials of the CeO_2 and CeO_2–AlN doping systems, oxidation in air from 900 to 1450 °C, and turning of tool steel with ceramic inserts of the same compositions were investigated to determine the effect of the N content of the intergranular phase. Si/N grain boundary diffusion was found to be the main controlling mechanism at high temperature for densification, mechanical behavior and chemical degradation of these materials in air, the passivation oxidation rate of the CeO_2–AlN–Si_3N_4 system being dependent on the atomic fraction of N of the intergranular phase, with lower values for the N-rich compositions.

1. Introduction

The densification of Si_3N_4 occurs by liquid phase sintering with the addition of different oxides or nitrides or mixtures of both, of which the CeO_2 and CeO_2–AlN doping systems are examples [1–4]. The low cost rare earth oxide CeO_2 is reported to give superior chemical resistance [5] and high fracture toughness [6]. Intergranular diffusion of Si and N is the controlling mechanism of densification, $\alpha \rightarrow \beta$-Si_3N_4 phase transformation and creep behavior [1, 7–11]. The chemical nature of the liquid phase is important for sintering, and for any property related to the liquid viscosity. The viscosity of the oxynitride glass is known to be enhanced by the N content and to be dependent on the glass-modifying cations [12–14].

In the present study the effect of N content on the sintering kinetics is correlated with two properties which are directly relevant to the use of Si_3N_4 as cutting tool inserts: the hot hardness [15–17] and oxidation resistance [18, 19].

2. Materials and experiments

Dense Si_3N_4 samples were uniaxially hot pressed at 20–30 MPa applied pressure, for 300–5400 s at 1500–1750 °C. Two samples were post-HIPed at 1750 °C for 1 h at 100 MPa. The phase composition, intergranular phase volume and N content of each batch are given in Table 1. The volume fraction of intergranular phase and N content were calculated from the amount and composition of sintering aids and the density of glasses of similar compositions [4].

TABLE 1. Composition of Si_3N_4-based materials, volume content and nitrogen content of corresponding intergranular phases

Batch	Composition (mol.%)				Intergranular phase	
	Si_3N_4	SiO_2	Ce_2O_3	AlN	Volume fraction V_L (%)	N-content[a] (at.%)
1Ce	88.8	10.2	1.0	—	7.5	—
2Ce	87.4	10.6	2.0	—	9.2	—
3Ce	84.6	11.4	4.0	—	12.8	—
1CeAl	76.2	7.3	0.9	15.6	10.1	27.1
2CeAl	73.2	7.5	1.8	17.5	12.6	26.3
3CeAl	69.0	8.0	3.5	19.5	16.9	24.2

Raw materials: Si_3N_4, HcStarck LC10 for batches 1–3Ce and HcStarck LC12 for batches 1–3CeAl; CeO_2, Fluka puriss; AlN, HcStarck grade C.
[a]From added AlN.

0921-5093/93/$6.00

The experimental procedures for hot-pressing dilatometry, hot-hardness testing and turning tests are reported elsewhere [15, 20, 21]. Oxidation tests were done in air [22] at 900–1450 °C for 0.5–25 h.

3. Results and discussion

3.1. Hot-pressing kinetics

Shrinkage data of pressure dilatometry in the range 1300–1800 °C were analyzed by non-linear curve fitting to a general densification equation which is based on Coble's equation [23] for the intermediate stage of sintering by a grain boundary diffusion mechanism, with an additional contribution of particle rearrangement in the early stages of the process [20, 24]. The effects of initial particle size and purity of the powders, of the sintering aid composition (either Ce^{3+}, Al^{3+}, N^{3-} or Mg^{2+}), and of the liquid volume fraction V_L, on the densification rate and α–β Si_3N_4 phase transformation and grain coarsening during sintering were analyzed and discussed separately [20, 24]. The full set of densification parameters for each of the batches in Table 1 is published elsewhere [20]. The values of effective diffusion coefficient, $D = D_0 \exp(-Q/RT)$, were calculated after correcting the densification rate for dependences on porosity, grain size and intergranular layer thickness. The values of D, V_L and relative N content are retained for comparison with the passive oxidation rate constants and the changes in hot hardness.

The values of D_0 and Q are dependent on the sintering aid, CeO_2, CeO_2–AlN or MgO–AlN, but are independent of the amount of each compound, Table 2. The differences in D_0 and Q between the three sets of batches of this study have been explained on the basis of the compensation law [24, 25]: $\ln D_0 = Q/RT^* + \ln B$, where $B = 4.9 \times 10^{-17}$ m^2 s^{-1}, $T^* = 1740$ K is a value of T in the center of the temperature range of the hot-pressing experiments, and the correlation coefficient is $c = 0.992$. The diffusion coefficients of N and Si in Si_3N and the effective diffusion coefficients of hot-pressing of Si_3N_4 have been reviewed [11]. The straight line for the compensation law joins the experimental points (D_0, Q) of hot-pressing of MgO-doped Si_3N_4 [8] and Y_2O_3–SiO_2-doped Si_3N_4 [9], and the diffusion coefficient of N in β-Si_3N_4, $D = 1.4 \times 10^7 \exp(-778$ kJ mol$^{-1}/RT)$ m^2 s^{-1} [11]. Since the values of D fit a single straight line, the same diffusion species must be controlling the solution–precipitation mechanism of densification of several Si_3N_4 materials, so the species responsible for the effective values of the Si/N diffusion coefficient is the N ion. Differences in the values of Q in Table 2 are explained as the effect of sintering aids on reactions that bring the solution–preparation of Si_3N_4 in the liquid to equilibrium. Dissolved N from the Si_3N_4 powder, or intentionally added as AlN, lowers the eutectic point of the system [4, 24, 26, 27]. A transient liquid, which recrystallizes as $CeAlO_3$ on cooling, is already observed at 1300 °C during hot pressing of the CeAl systems [24]. Transient liquids of analogous compositions were reported in Y–Si–Al–O–N [28, 29]. The batches 1–3 CeAl have lower values of Q, owing to the early contribution of the transient liquid to the hot pressing rate.

3.2. Hot hardness

The hot hardness results show that the N-rich compositions (batches 1–3CeAl), have high H_V values at room temperature which are retained up to 900 °C,

TABLE 2. Diffusion coefficient for densification and passive oxidation rate constant

Batch	Effective diffusion coefficient hot-pressing		Passive oxidation (1050–1350 °C in air)	
	D_0 (m^2 s^{-1})	Q (kJ mol^{-1})	K_0 (mg^2 cm^{-4} h^{-1})	Q_{ox} (kJ mol^{-1})
1Ce	1.2×10^{-2}	504	1.1×10^{11}	422
2Ce	1.8×10^{-2}	471	2.4×10^{11}	422
3Ce	1.6×10^{-2}	481	4.4×10^{11}	422
Average	1.5×10^{-2}	485		
1CeAl	1.6×10^{-6}	337	1.8×10^{13}	455
2CeAl	1.8×10^{-6}	385	1.1×10^{14}	455
3CeAl	1.4×10^{-6}	337	1.3×10^{15}	455
Average	1.6×10^{-6}	353		
MgAlG[a]	2.8×10^{-4}	412	—	—
MgAlF[b]	3.1×10^{-4}	425	—	—
Average	3.0×10^{-4}	418.5		

[a] 97.5% Si_3N_4 (HcStrack LC10) + 1% MgO (Merck puriss.) + 1.5% (weight per cent) AlN.
[b] 97.5% Si_3N_4 (HcStrack LC12) + 1% MgO + 1.5% AlN (weight per cent).

while H_V for batches 1–3Ce has a more pronounced dependence on T [15]. Two temperature ranges of H_V are observed. The values of the activation energy of H_V, in the range from room temperature (RT) to 800–900 °C, amount to 2.5–5.1 kJ mol^{-1} and 0.6–3.4 kJ mol^{-1} for 1–3Ce and 2–3CeAl respectively [24, 30]. The corresponding values of the activation energy of H_V in the high temperature range Q_H are given in Table 3. The values of Q_H of the 2CeAl samples are proportional to the logarithm of their room temperature hardness, Table 3. This proportionality is understood as resulting from competition, in the range 900–1200 °C, between the low and high temperature yielding mechanisms that relate to hardness [24, 30].

When the compensation law is applied to the reciprocals of H_V of the 2CeAl samples, to separate tentatively the contributions of the deformation mechanisms of Si_3N_4, a single value of activation energy, $Q_e = 49.5$ kJ mol^{-1}, is calculated for the high temperature mechanism of hardness of Si_3N_4, Table 3. This has been identified as grain boundary viscous flow [17], the hardness being related to the flow rate equations as $H^{-n} = [K'\exp(-Q/R)]t$, where K' is a constant which includes the pre-exponential factor of D, t is the indentation time and $n \geqslant 8$ [17]. By multiplying Q_e by $n = 8$, a value that is almost identical with Q, the activation energy of hot-pressing for the same batch (Table 2), is obtained ($nQ_e = 396$ kJ mol^{-1}). A relative increase in K^* from batch 3CeAl (K_3^*) to batch 2CeAl (K_2^*), $n \ln(K_2^*/K_3^*) = 2.5$, at $Q_H \approx 20$ kJ mol^{-1}, is observed. The intergranular phase of batch 2CeAl has a higher N-content than that of batch 3CeAl, Table 1.

The wear resistance of ceramics in dry friction is a function of their hardness H, toughness K_{Ic}, and the chemical stability of the ceramic to the second material of the sliding couple. Abrasion and chemical dissolution are competing mechanisms of wear for Si_3N_4 ceramics under high speed sliding contact with metals and alloys [21]. The abrasion wear resistance becomes proportional to $K_{Ic}^a H^b$, where $a \approx 2/3$ and $b \approx 1/2$ are real and positive constants [15]. The exact values of a and b are dependent on the mechanical properties, the microstructure of the two materials of the sliding couple, the test conditions and the kinetics of the tribological contact. The room temperature indentation toughness K_{Ic} is $K_{Ic} = 4.2 \pm 0.3$ MPa m$^{1/2}$ for the 2Ce cutting insert material and $K_{Ic} = 4.3 \pm 1.0$ MPa m$^{1/2}$ for the 2CeAl inserts [21]. For the dense Si_3N_4 materials, K_{Ic} is almost independent of T up to 1000 °C [31]. A net increase in K_{Ic} can be observed in the range 1000–1200 °C for those materials of high liquid volume fractions [31]. As discussed above, the effects of T on H_V are large and dependent on material composition. The specific wear resistance of the Ce-doped Si_3N_4 inserts to abrasion in cutting of iron alloys are improved by N enrichment of the intergranular layer [15, 21]. The rake face of the CeO_2–AlN–Si_3N_4 inserts (2CeAl) remains stable at cutting speeds of 2.5–4 m s^{-1}, whereas an extensive abraded crater is already observed in the CeO_2–Si_3N_4 material (2Ce) [21]. The relationship between wear resistance, cutting speed and hot hardness $H_V(T)$, was amenable to quantification [15]. The dissolution rate of Si_3N_4 in the chips of different iron alloys also shows that the N-rich compositions can survive at high cutting speeds for longer times [21].

3.3. Oxidation in air

The oxidation of CeO_2 and CeO_2–AlN doped Si_3N_4 in air reveals three temperature ranges [22]: (i) non-protective oxidation for $T < 1050$ °C, (ii) passivation at 1050–1350 °C and (iii) oxidation with extensive dissolution of the Si_3N_4 grains above 1350 °C. The oxidation rate K in range (i) is limited by the porosity of the reaction products and it decreases as T approaches 1050 °C. Range (iii) was only observed for the 2CeAl and 3CeAl HIP samples. The passive oxidation, range (ii), follows the parabolic law $W^2 = K(T)t$, where W is the weight gain and $K(T) = K_0 \exp(-Q_{ox}/RT)$, is the oxidation rate constant, Table 2. Within the experimental error of the present results (± 30 kJ mol^{-1}) Q_{ox} is constant for all batches, being almost identical with the value Q for densification of the CeO_2 doped batches, Table 2. Within ± 50 kJ mol^{-1}, the value of

TABLE 3. Room temperature hardness and hot hardness, $H = K^* \exp(Q_H/RT)$, of the Si_3N_4–CeO_2–AlN systems

Batch	Sample	H_V-RT (kgf mm^{-2})	900–1200 °C		
			K^* (kgf mm^{-2})	Q_H (kJ mol^{-1})	Q_e (kJ mol^{-1})
2CeAl	1500 °C, 60 min	2014	131	24.7	51.6
	1550 °C, 60 min	1958	160	21.8	52.9
	1600 °C, 60 min	1864	238	17.6	46.0
	1750 °C, 15 min	1700	316	13.1	47.5
3CeAl	1650 °C, 5 min	1598	134	20.5	—
	HIP	1526	56	28.7	—

Q_{ox} is also close to the values of activation energy of passive oxidation of several other Si_3N_4 materials with dopants of MgO [32, 33], CeO_2 [32] and Y_2O_3–Al_2O_3 [34]. For batches 1–3Ce, the increase in K_0 is directly proportional to V_L, Tables 1 and 2. The same proportionality was reported for the oxidation of MgO-doped hot-pressed Si_3N_4 [35]. The oxidation kinetics of Si_3N_4 and related nitrogen ceramics has been reviewed [36]. The mechanism of passive oxidation of Si_3N_4 and sialon in range (ii) has been described [35] as rate controlled by the outward diffusion of N and cation impurities and the inward diffusion of oxygen, along the grain boundaries in the subscale region. The linear relationship between K_0 and V_L is also proportional to the fractional area of intergranular phase of the surface, which is the area for diffusion of N and cations from the bulk of the Si_3N_4 to the reaction interface, the effective diffusivity being independent of the CeO_2 concentration in the intergranular liquid [37], Tables 1 and 2. For batches 1–3CeAl, K_0 has an exponential dependence on the atomic fraction of N of the intergranular phase, the correlation coefficient being 0.986 for $\ln(K_0) \propto N(\text{at.\%})$. The quality of the linear fit is further improved if $\ln(K_0)$ is plotted as a function of the molar ratio of AlN to $(AlN + Ce_2O_3)$ in the sintering aids, being $c = 0.999$, Fig. 1.

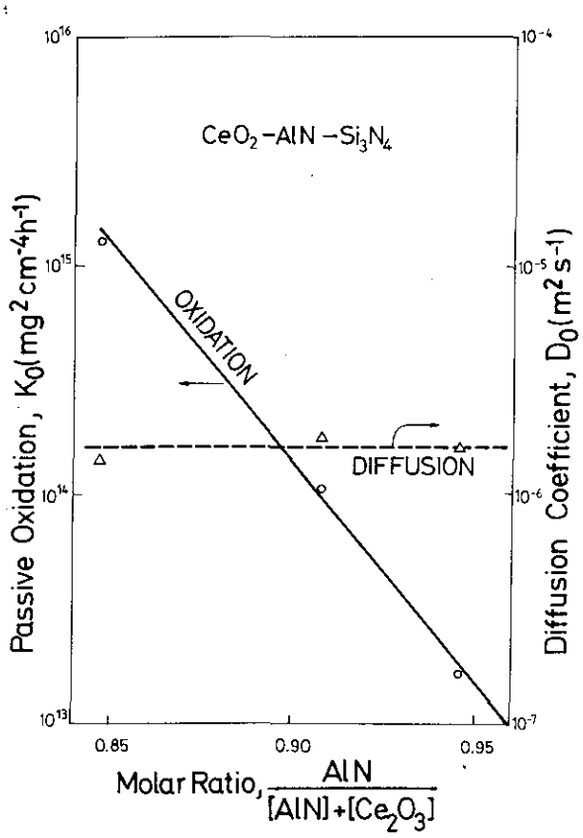

Fig. 1. Effect of AlN content on the pre-exponential factors of the diffusion coefficient in hot pressing and the passive oxidation rate constant.

Intergranular film thicknesses of 1.8–3.3 nm were calculated [20] for the samples in Table 2. The low atomic number of N, the limiting energy resolution and spatial resolution of existing equipment for surface analysis (Auger electron spectroscopy) and of analytical electron microscopy preclude the accurate determination of the N content in the intergranular films of Si_3N_4 [38]. An N content of 15 at.% was determined by electron energy loss spectroscopy in the grain boundary liquid phase of MgO-doped Si_3N_4 hot pressed at 28 MPa at 1500 °C for 2 h [38]. The calculated values of N content in Table 1 are above the reported saturation values of N concentration in N-containing glasses [39, 40], which increases from 15 at.% at 1650 °C and 0.1 MPa of N_2 pressure [39] to about 25 at.% at 1900 °C, 210 MPa of N_2 pressure [40]. The N content of the glasses is dependent on composition, glass melting temperature and time [14]. When reactive N sources, such as NH_3, are used as the atmosphere for melting the glass, the N content is also increased (20 at.%) [14]. In uniaxial hot pressing, the Si_3N_4 samples are highly confined by the dye walls, N losses for the short hot-pressing cycles at 1500–1750 °C being minimal. Except for the transient $CeAlO_3$, no secondary crystalline phases were detected by X-ray diffraction in the CeAl hot pressed samples, Table 2. Most of the N, added as AlN, remained in the sintering liquid in amounts that must be proportional to the dissolved AlN.

The substitution degree of β'-Si_3N_4 in the CeAl samples is below the detection limit of X-ray diffraction [24]. Al from AlN enters the liquid in the same amount as the N. The oxidation rate of sialons either decreases or increases when the Al content increases [36]. K decreases one order of magnitude at 1370 °C, from 2.36×10^{-12} g^2 cm^{-4} s^{-1} to 2.22×10^{-13} g^2 cm^{-4} s^{-1}, in sialons when the weight fraction of Al_2O_3 is increased from 20 wt.% to 50 wt.% [41]. The relative change in Al content of the CeAl samples in Tables 1 and 2 is much lower than these values.

The increase in K_0 from batch 2CeAl to batch 3CeAl, Table 2, is given as $\ln(K_0^{(3)})/K_0^{(2)}) = 2.45$, which is the same as the relative change in $n \ln K^*$ above. The substitution of N for O increases the average anion coordination number which leads to glass network cross-linking, high viscosities, lower diffusion coefficients and better high temperature resistance of the material [12–14]. The exponential dependence of viscosity of the oxynitride glasses on e/oN = 3N(at.%)/[3N(at.%) + 2O(at.%)], the equivalent concentration of N in the glasses [12–14], can explain the exponential relationship observed for K_0, Fig. 1.

4. Conclusions

The activation energy for densification Q, grain boundary viscous flow of hot hardness nQ_e and passive oxidation rate in air Q_{ox} of CeO_2–AlN doped Si_3N_4 are virtually the same, these phenomena all being controlled by the same diffusional mechanism. The effective diffusion for hot pressing is coupled to N diffusion in Si_3N_4.

In overlapping temperature ranges, below the hot pressing temperatures, the yielding rate of hot hardness and the passive oxidation rate of the CeO_2–AlN doped Si_3N_4 have identical relative increments with increasing N content, the oxidation rate being exponentially dependent on the AlN molecular fraction of the sintering aids.

The hot hardness and oxidation, being also controlled by diffusion in the intergranular phase, show similar trends to the wear resistance of Si_3N_4 cutting inserts as a function of N content.

Acknowledgments

The financial support from JNICT and Minas e Metalurgia under the research contract 87/80 MATR is gratefully acknowledged.

References

1 G. N. Babini, A. Bellosi and P. Vincenzini, *Ceram. Int., 6* (3) (1980) 91–98.
2 T. Mah, K. S. Mazdiyasni and R. Ruh, *J. Am. Ceram. Soc., 62* (1–2) (1979) 12–16.
3 F. F. Lange, *Am. Ceram. Soc. Bull., 59* (2) (1980) 239–240, 249.
4 J. Mukerji, P. K. Das, P. Greil and G. Petzow, *Ceram. Int., 13* (1987) 215–221.
5 S. T. Buljan and S. F. Wayne, *Adv. Ceram. Mater., 2* (4) (1987) 813–816.
6 E. Tani, S. Umebayashi, K. Kishi, K. Kobayashi and M. Nishijima, *Am. Ceram. Soc. Bull., 65* (9) (1986) 1311–1315.
7 R. J. Brook, T. G. Carruthers, L. J. Bowen and R. J. Weston, in F. Riley (ed.), *Nitrogen Ceramics*, Noordhoff, Leyden, 1977, pp. 383–390.
8 L. J. Bowen, R. J. Weston, T. G. Carruthers and R. J. Brook, *J. Mater. Sci., 13* (1978) 341–350.
9 L. J. Bowen, T. G. Carruthers and R. J. Brook, *J. Am. Ceram. Soc., 61* (7–8) (1978) 335–339.
10 O. Abe, *J. Mater. Sci., 25* (1990) 4018–4026.
11 G. Ziegler, J. Heinrich and G. Wotting, *J. Mater. Sci., 22* (1987) 3041–3086.
12 S. Hampshire, R. A. Drew and K. H. Jack, *Commun. Am. Ceram. Soc., 67* (1984) C-46–C-47.
13 R. A. Drew, S. Hampshire and K. H. Jack, *Proc. Br. Ceram. Soc., 31* (1981) 119–132.
14 R. E. Loehman, *J. Mater. Educ., 9* (5) (1987) 483–498.
15 R. Silva and J. Vieira, *J. Hard Mater., 3* (1) (1992) 63–72.
16 T. Ekstrom and J. Persson, *J. Am. Ceram. Soc., 73* (10) (1990) 2834–2838.
17 M. G. Naylor and T. F. Page, *Tech. Rep., DA-ERO-78-G-010*, University of Cambridge, 1981.
18 E. M. Trent, *Metal Cutting*, Butterworths, Guildford, 1984.
19 J. A. Schey, *Tribology in Metalworking*, American Society for Metals, Metals Park, OH, 1983.
20 R. Silva and J. Vieira, *Proc. European Ceramic Society Second Conf., Augsburg, 1991*, Deutsche Keramische Gessellshaft, Koln, in press.
21 R. Silva, J. Gomes, A. Miranda and J. Vieira, *Wear, 148* (1991) 69–89.
22 A. P. Moreira, Estabilidade química e tempo de vida no sistema Si–Ce–Al–O–N a temperaturas elevadas, *MSc Thesis*, University of Aveiro, Portugal, 1992.
23 R. L. Coble, *J. Appl. Phys., 41* (12) (1970) 4798–4807.
24 R. Silva, Cinética de sinterização e desgaste de pastilhas de corte do sistema Si_3N_4–CeO_2–AlN, *PhD Thesis*, University of Aveiro, Portugal, 1992.
25 J. M. Vieira and R. J. Brook, in W. D. Kingery (ed.), *Advances in Ceramics*, Vol. 10, American Ceramic Society, Columbus, OH, 1983, pp. 438–463.
26 K. H. Jack, in P. Vincenzini (ed.), *Energy and Ceramics, Materials Science Monographs*, Vol. 6, Elsevier, Amsterdam, 1980, pp. 534–549.
27 P. K. Das and J. Mukerji, *Key Engineering Materials*, Vol. 29–31, Trans Tech Publications, Aedermannsdorf, 1989, pp. 109–120.
28 P. K. Das and J. Mukerji, *J. Eur. Ceram. Soc., 5* (1989) 105–112.
29 J. Mukerji, P. Greil and G. Petzow, *Sci. Sintering, 15* (1) (1983) 43–53.
30 R. Silva and J. Vieira, Hot-hardness of Si_3N_4-based cutting tools, to be published.
31 B. S. Karunaratne and M. H. Lewis, *J. Mater. Sci., 15* (1980) 449–462.
32 D. Cubiccioti and K. H. Lau, *J. Am. Ceram. Soc., 61* (11–12) (1978) 512–517.
33 S. C. Singhal, *J. Am. Ceram. Soc., 59* (1–2) (1976) 81–82.
34 T. Chartier, J. L. Besson and P. Goursat, *Int. J. High-Technol. Ceram., 2* (1986) 33–45.
35 D. R. Clarke and F. F. Lange, *J. Am. Ceram. Soc., 63* (9–10) (1980) 586–593.
36 C. C. Sorrell, *J. Aust. Ceram. Soc., 19* (2) (1983) 48–67.
37 T. Ekstrom and M. Nygren, *J. Am. Ceram. Soc., 75* (2) (1992) 259–276.
38 D. R. Clarke and N. J. Zaluzec, *Commun. Am. Ceram. Soc., 65* (1982) C-132–C-133.
39 D. R. Messier and A. Broz, *Commun. Am. Ceram. Soc., 65* (1982) C-122–C-123.
40 J. C. Mittl, R. L. Tallman, P. V. Kelsey, Jr. and J. G. Jolley, *J. Non-Cryst. Solids, 71* (1985) 287–294.
41 S. C. Singhal and F. F. Lange, *J. Am. Ceram. Soc., 60* (3–4) (1977) 190–191.